Accepted Manuscript

Syntheses of U_3O_8 nanoparticles form four different uranyl complexes: their catalytic performance for various alcohol oxidations.

Ishani Majumder, Sourav Chatterjee, Roland C. Fischer, Swarup Kumar Neogi, Franz A. Mautner, Tanmay Chattopadhyay
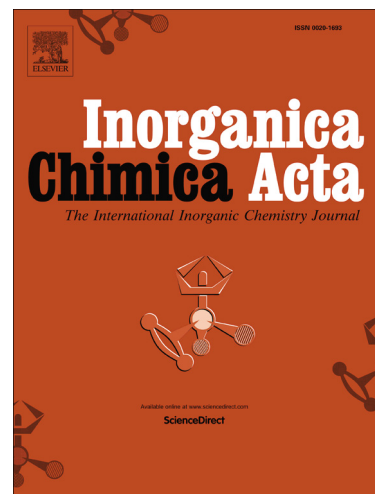
Please cite this article as: I. Majumder, S. Chatterjee, R.C. Fischer, S.K. Neogi, F.A. Mautner, T. Chattopadhyay, Syntheses of U_3O_8 nanoparticles form four different uranyl complexes: their catalytic performance for various alcohol oxidations., *Inorganica Chimica Acta* (2017), doi: http://dx.doi.org/10.1016/j.ica.2017.03.020

Syntheses of U_3O_8 nanoparticles form four different uranyl complexes: their catalytic performance for various alcohol oxidations.

Ishani Majumder,[a] Sourav Chatterjee,[b] Roland C. Fischer,[c] Swarup Kumar Neogi,[d] Franz A. Mautner,[*,e] Tanmay Chattopadhyay,[*,b]

[a] Department of Chemistry, University of Calcutta, 92 A. P. C. Road, Kolkata-700 009, India

[b] Department of Chemistry, Panchakot Mahavidyalaya, Sarbari, Purulia, Pin-723121, India, E-mail: tanmayc2003@gmail.com

[c] Institut fuer Anorganische Chemie, Technische Universitaet Graz, A-8010 Graz, Austria.

[d] Department of Physics, Adamas University, Barasat Barrackpore Road, P.O. Jagannathpur, Kolkata-700126, West Bengal, India

[e] Institut fuer Physikalische and Theoretische Chemie, Technische Universitaet Graz, A-8010, Graz, Austria, E-mail: mautner@tugraz.at

ABSTRACT

Two Dinuclear complexes namely $[(UO_2)_2(L1)_2(DMSO)_2]$ (**1**) and $[(UO_2)_2(L2)_2(DMSO)_2]$ (**2**) of two Schiffbase ligands 2-[(2-Hydroxy-3-methoxy-benzylidene)-amino]-2-hydroxymethyl propane-1,3-diol (HL1) and 2-[(3,5-Dichloro-2-hydroxy-benzylidene)-amino]-2-hydroxymethyl-propane-1,3-diol (HL2) obtained by condensation of the aldehydes 2-Hydroxy-3-methoxy-benzaldehyde and 3, 5-Dichloro salicylaldehyde with Tris(hydroxymethyl)aminomethane ammine, have been synthesized. On the other hand, when the two aldehydes were treated with uranyl nitrate two mononuclear complexes, $[(UO2)(L3)_2(DMSO)_2]$ (**3**) and $[(UO2)(L4)_2(DMSO)_2]$ (**4**), are obtained. The complexes are then heated at 800°C in open atmosphere to obtain the U_3O_8 nanomaterials as the final product. X-ray diffraction (XRD), scanning electron microscopy (SEM), and transmission electron microscopy (TEM) were employed to characterize the so obtained the U_3O_8 nanoparticles. Studies shows the synthesized U_3O_8 nanoparticles obtained from different complexes were different as far as morphology and size are concerned. All four different U_3O_8 nanoparticles explored as

oxidising catalyst to oxidize alcohols where morphology of the nanoparticles controls the catalytic efficiency.

Keywords: Schiff-base; Uranyl nitrate; Nanoparticles,Alcohol Oxidation, Morphology dependent catalysis

1. Introduction

An unusual and remarkable characteristic of metal oxide nano particles is that their surface energies per unit volume can be easily tuned or controlled just by slight modification in thermal and chemical conditions. Therefore synthesis of these nanoparticles having various phases and morphologies has become prime interest to interest to researchers, as it is possible to direct the physical/chemical properties of these materials just by regulating their phase and morphology. As a result they have vast and potential applications in various fields like optics, electronics, magnetics, and catalysis[1]. Among the above mentioned fields, here we are specially interested towards the application of nano materials as catalyst because catalysts are the vital requirement for proficient conversion of raw materials into different essentials of modern livelihood. And also nano materials can be considered as potential catalyst due to their active surface and interfacial atom effect, high reactivity, low catalyst loading, environmentally gentle nature, easy recovery and reusability [2-11]. Here we have chosen Uranium as the metal for the preparation of metal oxide nano particles because it may demonstrate ways for re-consumption of vast amount of depleted uranium, resulted from enrichment manufacture[12-14].Although there are plenty of reports in literature that uranium oxide nanoparticles can exhibit admirable catalytic actions for demolition of volatile organic compounds (VOCs) and for selective reduction of NO at suitable temperatures[12,15-16], but there are lack of information for using it in catalytic purposes in synthetic chemistry [17]. Also the reported synthetic procedure for Uranium oxide nano particles are infrequent in comparison with main group elements,3d elements or 4f elements. All of this lack of investigations therefore motivated us towards our present work where we synthesize the uranium oxide nanoparticles by very simple but effective manner just by employing the pyrolytic reaction to our four synthesized complexes $[(UO_2)_2(L1)_2(DMSO)_2]$ (**1**), $[(UO_2)_2(L2)_2(DMSO)_2]$ (**2**), $[(UO_2)(L3)_2(DMSO)_2]$ (**3**), $[(UO_2)(L4)_2(DMSO)_2]$ (**4**). Where the ligands L1 and L2 are Schiff bases and L3 and L4 are their corresponding aldehydes. Interestingly, all of the

complexes give U_3O_8 nanoparticles with various morphologies as the end product of the pyrolytic reaction. The synthesis, characterization of the metal complexes and metal oxide nanoparticles and the morphology dependent catalytic oxidation of the nanoparticles towards aromatic alcohols are vividly portrayed in this manuscript.

Scheme 1.

2. Experimental Section

2.1. Physical Methods and Materials.

The chemicals used for this work were purchased from commercial agencies and used as obtained. Solvents were distilled and dried according to standard procedure before using in the experiment. Water used in all physical measurement and experiments was Milli-Q grade. 3,5-Dichloro salicylaldehyde, 2-Hydroxy-3-methoxy-benzaldehyde, Tris(hydroxymethyl)aminomethane, Benzyl alcohol and other alcohols were purchased from Aldrich and used in oxidation experiments without further purification. Uranyl nitrate hexahydrate was also purchased from Sigma.

PerkinElmer 240C analyzer was used for elemental analysis (carbon, hydrogen and nitrogen). Shimadzu FT-IR 8400S and PerkinElmer Spectrum Express Version was used for recording Infrared spectra (4000-400 cm^{-1}) using KBr pellets as mediums. Shimadzu UV-2450PC spectrophotometer with multiple cell-holders and thermostat were used to supervise the UV-visible spectra. Bruker AV300 Supercon NMR spectrometer was used for recording ^1H and ^{13}C NMR spectra (300 MHz) in $CDCl_3$ and using the solvent signal as the internal standard in a 5 mm BBO probe. Waters Xevo GT S Q-TOF mass spectrometer was used for recording the electrospray ionization mass spectra.

Mettler Toledo (TGA/SDTA851) thermal analyzer was used for thermo gravimetric analysis (TG-DTA) in flowing dinitrogen (flow rate: 30 $cm^3 min^{-1}$). JEOL JSM-6700F field-emission microscope was utilized to carry out the Field Emission Scanning Electron Microscopic (FE-SEM) measurement. JEOL (Japan) JEM2100 high-resolution transmission electron microscope was employed for Transmission Electron Microscopic (TEM) measurement. XPERT-PRO Diffractometer monochromated Cu-Ka radiation (40.0 kV, 30.0 mA) was used for X-ray powder diffraction (PXRD) at room temperature. Zetasizer Nano ZS; Malvern Instruments, Malvern, UK was used to execute dynamic Light Scattering experiments (DLS). Micromeritics Tristar 3000 surface area analyzer was utilized for the BET analysis.

2.2. Synthesis of the complex

For preparation of all the four complexes the subsequent common template synthetic procedures were taken on. Firstly the ligand solution were prepared in situ via condensation of 3,5-Dichloro-2-hydroxy-benzaldehyde and 2-Hydroxy-3-methoxy-benzaldehyde as the aldehydes with the corresponding amine as (Tris-(hydroxymethyl)aminomethane) with maintaining the same molar ratio and then the methanolic solution of uranyl nitrate hexahydrate was added in this mixture to obtain the complexes **1** and **2**. The other two complexes (*i.e* complex **3** and **4**) were prepared just by reaction with the aldedydes (HL3 and HL4) with uranyl nitrate hexahydrate solution. Their synthesis, composition and other physicochemical characteristics are specified underneath.

2.2.1 [(UO2)2(L1)2(DMSO)2] (*1*)

A methanolic solution (5 mL) of Tris(hydroxymethyl)aminomethane (91 μL,1 mmol) was added to a methanolic solution (5 mL) of 2-Hydroxy-3-methoxy- benzaldehyde (0.152 g,1 mmol) in a drop wise mode and the resulting solution was refluxed for about 30 mins. Then a methanolic solution (5 mL) of uranyl nitrate hexahydrate (0.502 g, 1 mmol) was added to this ligand and further refluxed for about 30 mins. The resulting dark orange colored solution was filtered and kept in a CaCl$_2$ desiccator. The crude product so obtained after evaporation of the solvent was collected, washed and further recrystalised in DMSO medium. The dark orange colored single crystals appropriate for the X-Ray diffraction were achieved from this recrystalisation procedure (yield 75%). Anal. Calcd for C$_{28}$H$_{42}$N$_2$O$_{16}$S$_2$U$_2$: C, 27.95; H, 3.49; N, 2.32. Found: C, 27.87; H, 3.86; N, 2.27. IR (KBr): ν(C=N) 1625 cm−1; ν (skeletal vibration) 1532 cm^{-1}; UV/vis (DMSO): $\lambda_{max/nm}$ (ε/dm^{3}mol^{-1}cm^{-1}) = 267(3676), $\lambda_{max/nm}$ (ε/dm^{3}mol^{-1}cm^{-1}) = 405(1778).

2.2.2 [(UO2)2(L2)2(DMSO)2] (*2*)

A methanolic solution (5 mL) of Tris(hydroxymethyl)aminomethane (91 μL,1 mmol) was added to a methanolic solution (5 mL) of 3,5-Dichloro-2-hydroxy benzaldehyde (0.191 g, 1mmol) in a drop wise mode and the resulting solution was refluxed for about 30 mins. Then a methanolic solution (5 mL) of uranyl nitrate hexahydrate (0.502 g, 1 mmol) was added to this ligand and further refluxed for about more 30 mins. The resulting dark orange colored solution was filtered and kept in a CaCl2 desiccator. The crude product so obtained after evaporation of the solvent was collected, washed and further recrystalised in DMSO medium. Which were further recrystalised from ethanol for purification of the compound (yield 70%). Anal. Calcd for C$_{26}$H$_{34}$N$_2$O$_{14}$S$_2$U$_2$Cl$_4$: C,

24.37; H, 2.65; N, 2.18. Found: C, 24.17; H, 2.86; N, 2.17. IR (KBr): ν(C=N) 1625 cm^{-1}; ν (skeletal vibration) 1512 cm^{-1}; UV/vis (DMSO): $\lambda_{max/nm}$ (ε/dm^{3}mol^{-1}cm^{-1})= 257(3338), $\lambda_{max/nm}$ (ε/dm^{3}mol^{-1}cm^{-1}) = 428(2233).

2.2.3 [(UO2)(L3)2(DMSO)2] (3)

A methanolic solution (5 mL) of uranyl nitrate hexahydrate (0.502 g, 1 mmol) was added in a drop wise mode to a methanolic solution (5 mL) of 2-Hydroxy-3-methoxy-benzaldehyde (0.152 g, 1 mmol) followed by 30 min reflux. The resulting dark red solution was then filtered and kept in a CaCl2 desiccator. The crude product so obtained after evaporation was collected, washed and further recrystalised in DMSO medium. Which were further recrystalised from ethanol for purification of the compound. Anal. Calcd for $C_{20}H_{26}O_{10}S_2U_1$: C, 32.96; H, 3.43; Found: C, 32.36; H, 3.22; IR (KBr): ν(C=N) 1695 cm^{-1}; ν (skeletal vibration) 1535 cm^{-1}. UV/vis (DMSO): $\lambda_{max/nm}$ (ε/dm3mol^{-1}cm^{-1}) = 264(3642), $\lambda_{max/nm}$ (ε/dm3mol^{-1}cm^{-1}) = 449(1303).

2.2.4[(UO2)(L4)2(DMSO)2](4)

A methanolic solution (5 mL) of uranyl nitrate hexahydrate (0.502 g, 1 mmol) was added in a drop wise mode to a solution (5 mL) of 3,5-Dichloro-2-hydroxy benzaldehyde (0.191 g, 1 mmol) followed by 30 min reflux. The resulting dark red solution was then filtered and kept in a CaCl2 desiccator. The crude product so obtained after evaporation was collected, washed and further recrystalised in DMSO medium. The dark red colored single crystals appropriate for the X-Ray diffraction were achieved from this recrystalisation procedure (yield 70%). Anal. Calcd for $C_{18}H_{18}O_8S_2U_1Cl_4$: C, 26.79; H, 2.23; Found: C, 26.87; H, 2.06; IR (KBr): ν(C=N) 1625 cm^{-1}; ν (skeletal vibration) 1532 cm^{-1}; UV/vis (DMSO): $\lambda_{max/nm}$ (ε/dm^{3}mol^{-1}cm^{-1}) = 262(4937), $\lambda_{max/nm}$ (ε/dm^{3}mol^{-1}cm^{-1}) = 429(1706).

2.3 Alcohol oxidation study of catalysts

To 1 mmol solution of the aromatic alcohol in EDC solvent, 1.25 mmol of PhI(OAc)$_2$ and 300 mg of the MgSO$_4$ along with 0.01 mmol of Uranium oxide nanoparticles were added. The mixture was stirred about 8 to 10 hrs at 45°C using TLC to monitor the sequence. After completion of the reaction, it was filtered, the solvent was then evaporated, the crude was purified by coloum chromatography and the final product was characerized by ^{1}H-NMR spectroscopy.

2.4. X-ray data collection and crystal structure determination:

The X-ray single-crystal data of compounds **1** and **4** were collected on a Bruker-AXS APEX-II CCD and Bruker-AXS microsource diffractometer. The crystallographic data, conditions retained for the intensity data collection and some features of the structure refinements are listed in Table 1. The intensities were collected with M_o-K_α radiation (λ= 0.71073 Å). Data processing, Lorentz-polarization and absorption corrections were performed using SAINT, APEX and the SADABS computer programs [18]. The structures were solved by direct methods and refined by full-matrix least-squares methods on F^2, using the SHELXTL [19] program package. All non-hydrogen atoms were refined anisotropically. The hydrogen atoms were located from difference Fourier maps assigned with isotropic displacement factors and included in the final refinement cycles by use of geometrical constraints. Molecular plots were performed with the Mercury [20] program with a version of 3.8.

CCDC 1500829-500830 contain the supplementary crystallographic data for this paper. These data can be obtained free charge from the Cambridge Crystallographic Data Centre via http://www.ccdc.cam.ac.uk/5datarequest/cif.

Table 1.

3. Results and Discussion

3.1. Synthesis, Rationalization, and Characterization of the Metal-Complexes

Complex **1** and **2** were prepared by general template synthetic procedure. Firstly the Schiff base ligands were synthesized by combining between 2-Hydroxy-3-methoxy-benzaldehyde(HL1), 2,5-Dichloro-2-hydroxy benzaldehyde (HL2) and the corresponding ammine (Tris(hydroxymethyl)aminomethane), then a methanolic solution of uranyl nitrate hexahydrate was added to obtain the complexes. On the other hand, complex **3** and **4** are synthesized just by treating the aldehydes with the methanolic solution of Uranyl nitrate. In some cases for complex **1** and **4** single crystals suitable for X ray diffraction analysis were obtained.

3.2. IR and UV-Visible Spectra of the complexes

The FTIR spectra of compounds **1-4** are shown in **Fig. S1-S4.** Complexes **1** and **2** show bands due to C=N stretch in the region 1625 cm^{-1} and complexes **3** and **4** show bands in the region of 1693-1695 cm^{-1} due aldehydic C=O stretch. All the complexes show skeletal vibration in the region

1516-1532 cm^{-1}. Electronic spectra of all the complexes have been studied in DMSO medium (**Fig. S5-S8**). Two distinct peaks have been recognized in all the cases. The first ones in the region of 257-267 nm which are due to the π-π* transition of the imine group [21]. The red-shifted peak around the region of 405-450 nm are due to the LMCT (5f of Uranium to Oxygen 2p) [21].

3.3. Solution studies: Mass Spectrometry

For better understanding of the solution phase structure or composition of the complexes Mass spectral study has been executed (Figures S9-S12). The spectral analysis reveals that complexes **1** and **2** exhibit similar solution structure as both of them shows a base peak at 564.1184 amu and 602.9757 amu respectively, which corroborates well with the dinuclear uranium species $[(UO_2)_2(L1/L2)_2(H_2O)_2].2Na^+$, (calc.m/z 564.0860 amu and 602.9640 amu respectively). Complexes **3** and **4** also behave similarly in solution and show the base peaks at 441.5513 and 497.8875 amu respectively which corroborates well with the mononuclear species $[(UO_2)(L1/L2)(H_2O)_2]^+$, (calc. m/z 441.5800 and 497.8860 amu respectively).

3.4. Crystal Structure Descriptions.

Single crystal structural analyses reveal that **1** consists of four crystallographically indipendent neutral centrosymmetric dinuclear $[UO_2(L1)(DMSO)]_2$ subunits, whereas **4** consists of mononuclear complexes $[UO_2(L4)_2(DMSO)_2]$. Since the four dinuclear $[UO2(L1)(DMSO)]2$ units in the unit cell have similar geometries (Table 2), we describe here only one dinuclear entity as representative (Fig. 1). In this complex the metal is coordinated by N(1) and six oxygen donor atoms. The UO_6N chromophore may be described as compressed pentagonal bipyramid with the uranyl oxygen atoms O(6) and O(7) located in the axial sites [U(1)-O(6) = 1.792(9), U(1)-O(7) = 1.813(10) Å, O(6)-U(1)-O(7) = 178.8(4)°]. The L1 ligand is chelating the U(1) via O(1) and N(1) donors [U(1)-O(1) = 2.278(7), U(1)-N(1) = 2.590(10) Å, O(1)-U(1)-N(1) = 69.6(3)°] and bridging U(1) and centrosymmetric U(1') [(') –x,2-y,1-z] via O(3) donor atom to generate the dinuclear subunit. The bond parameters within the four membered planar U_2O_2 ring are: U(1)-O(3) = 2.351(7), U(1)-O(3') = 2.341(7), U(1)…U(1') = 3.8930(7) Å, U(1)-O(3)-U(1)' = 112.1(3); O(3)-U(1)-O(3') = 67.9(3)°]. Coordination number seven is completed by O(8) donor atom of a terminal DMSO molecule located in equatorial site [U(1)-O(8) = 2.360(9) Å]. Oxygen atoms O(2), O(4) and O(5) of L1 molecule are not ligated to uranium centers, but are involved in hydrogen bonds of type O-H…O to generate a supramolecular 2D system oriented along the a- and b-axis of the triclinic unit cell (Table S1).

The equatorial sites of pentagonal bipyramid around U(1) of mononuclear complex **4** (Fig. 2) are occupied by O(1) and O(2) donor atoms of a chelating ligand molecule L2 [U(1)-O(1) = 2.314(2), U(1)-O(2) = 2.517(2) Å O(1)-U(1)-O(2) = 68.58(8)°], O(3) donor of a second L2 molecule which act only as terminal ligand [U(1)-O(3) = 2.308(2) Å], and O(5) and O(6) donor atoms of two terminal DMSO molecules [U(1)-(O5) = 2.367(2), U(1)-O(6) =2.402(2) Å]. The axial sites of the UO_7 chromophore are occupied by the uranyl oxygen atoms O(7) and O(8) [U(1)-O(7) = 1.779(3), U(1)-O(8) = 1.785(3) Å, O(7)-U(1)-O(8) = 175.73(11)°] (Table 3).

Table 2.

Fig. 1

Table 3.

Fig. 2

3.5. Synthesis, Rationalization, and Characterization of the Metal-Oxide Nanoparticles.

3.5.1. Synthesis of U_3O_8 Nanoparticles.

For the typical preparation of U_3O_8 nanoparticles, all the four complexes (**1-4**) were placed inside in a Teflon lined stainless steel autoclave sealed in platinum crucible and heated for 3 hr at 800ºC temperature. After 3 hr the crucible was left to cool at room temperature. After cooling the final product was collected and washed a number of times with ethanol and vacuum dried.

3.5.2. Characterization of the Nanoparticles.

3.5.2.1. Thermogravimetric Analysis.

Thermogravimetric analysis was employed to evaluate the thermal behavior of the complexes which are used as precursors of the nanoparticles. Detailed analysis of the thermogramms (**Fig. S15a**) reveal that Complex **1** and **2** gives U_3O_8 as stable end product directly as evident from the pyrolytic reaction [exp.weight loss = 29.93% (calcd 29.95%) for complex **1]** and [exp. weight loss = 36.24% (calcd 34.21%) for complex **2**]. But for Complex **3** and **4** the end product of the thermal reaction is the UO_2 nano particles as evident from the TG diagram (**Fig. S15b**) [exp.weight loss = 59.26% (calcd 61.21%) for complex **3** and [exp. Weight loss = 65.24% (calcd 66.34%) for complex **4**]. The UO_2 nano particles so formed is then readily transformed into U_3O_8 nano particles through

thermal treatment in air as we have kept the Platinum crucible in 800°C for few hours in the preparation of nano particles. Because of the high temperature the nano crystalline UO_2 particles re-crystallize and further oxidized into the more stable U_3O_8 form, as reported by other groups [17, 22-23]

3.5.2.2. Powder X-ray Diffraction Analysis.

The nanoparticles are named as UNP1, UNP2, UNP3 and UNP4 according to their synthetic precursors respectively. **Fig. 3** corresponds to the XRD patterns of all the U_3O_8 compounds. It reveals that all of the samples are polycrystalline in nature. The observed peaks in this XRD pattern corroborates well with those of the orthorhombic α-U_3O_8 structure[24]. It is reported in literature that U_3O_8 exists as mixed-valent Uranium (V/VI) compound in a molar ratio of 2 : 1. In general, the compound U_3O_8 crystallizes into three different polymorphs: (i) conventional orthorhombic α-U_3O_8 and two high- temperature variations (ii) hexagonal U_3O_8 (iii) orthorhombic β-U_3O_8[25-26]. However, in the present work, the peaks observed in the XRD pattern represented in Fig. 3 can be indexed with that of orthorhombic α-U_3O_8 structure[26]. So, in contrast with the reported XRD pattern of the orthorhombic α-U_3O_8 [21] the XRD pattern of our compound UNP1 (U_3O_8) demonstrates almost comparable intense (001) and (130) reflections. But for the other two compounds U_3O_8 (UNP2) and U_3O_8 (UNP3), (001) reflection is comparatively more intense than the other (130) peak, suggesting these two compounds [U_3O_8 (UNP2) and U_3O_8 (UNP3)] the particles are preferentially oriented along a definite direction. However, in case of U_3O_8 (UNP4), intensities of the (001) and (130) reflections are equivalent along with some additional reflections (highlighted in the **Fig. 3**). Those additional reflections do not match with reflections of β-U_3O_8 and γ-U_3O_8 phases; hence we can conclude that these reflections are due to another α-U_3O_8 phase with somewhat different lattice constants. As no additional peaks of impurity have been found in the entire XRD pattern, signifies that the obtained nano-crystalline U_3O_8 via this synthesis method are absolutely pure in nature. Moreover, it is evident from the XRD pattern that the broadening of the diffraction peaks indicates small size of the particles in these compounds [27].

Fig. 3

3.5.2.3. Scanning Electron Microscopy Analysis.

The Scanning electron microscopic (SEM) analysis helps us to evaluate the morphology and particle size of the metal oxide nanoparticles so prepared (**Fig. 4**). It is evident from the micrograph that the nano materials exist in different morphological shapes with an average size range of 50-100 nm. Detail assessment of the micrograph reveals that UNP1 have irregular shape morphology, while UNP2 have very small granule like structure. UNP3 have particle like morphology whereas UNP4 have distinct petals like structure. The roughened edges of the surface of the particles as noticed from the respective SEM images indicating the slow growth of the nano particles by a process of oriented accumulation of small primary nanocrystals.

Fig. 4

3.5.2.4. Dynamic Light Scattering.

Dynamic light scattering experiment was carried out to determine of the hydrodynamic size of the NPs. The representative DLS graph so obtained, indicates the formation of stable and non aggregated particles with a mean diameter of 70±20 nm and 50±20 nm for all U_3O_8 (UNP1,UNP2,UNP3 and UNP4)nanoparticles respectively (**Fig. 5**). Thef our types of nano particles (UNP1, UNP2, UNP3 and UNP4) are indexed with the PDI values of 0.616, 0.465, 0.515, 0.475 respectively. The estimated size distribution histograms (**Fig. 5 and Fig. S16**) and the PDI values authenticated their size distribution and good stability in water respectively.

Fig. 5

3.5.2.5. Transmission Electron Microscopy Analysis.

Transmission Electron Microscopic analysis were performed to obtained the actual size *i.e* the diameter of the nano particles in solid state. Thorough examination of the TEM images in Fig. 6 of the four nano particles demonstrates that all the nano particles exhibit nearly spherical geometry. UNP1, UNP3 and UNP4 nano particles display a mean size of 30±10 nm. Whereas for UNP2, the average diameter becomes smaller compared to the other and exhibits a diameter of 5±2 nm. Both the TEM and DLS experiments measure the diameter of the nano particles, but the diameter obtained from TEM analysis is found to be quite smaller with respect to the diameter obtained from DLS, which is quite obvious as TEM analysis gives the size of the nano's in dried state whereas, DLS gives the hydrated diameter. Actually, from the Transmission electron microscopy, the images we obtained

is for single particle, whereas for DLS gives the hydrodynamic diameter which is biased toward the larger-size end of the population distribution.

Fig. 6

3.5.2.6. Energy-Dispersive X-ray Spectroscopy.

EDX spectrum of the NPs are represented in **Fig. S17 and S18**.U and O signals come from the U_3O_8 nanoparticles. Small signals of other elements are due to presence of those elements in water. And for UNP3 the EDX spectrum gives a signal of copper which is due to the copper grid. The Platinum (Pt) signals come from the coating material of the instrument.

3.6. Catalytic Oxidation of Alcohols.

Fractional oxidation of benzyl alcohol in various solvent employing UOx/MCM-41 materials as the catalyst has been previously reported.[28] But incorporation of these solvents in the catalytic reaction produces by-products in the reaction system and thereby it is becoming hard to separate the preferred material from the solvent. To avoid this complication in product separation and to minimise the formation of by-products, solvent-free conditions are employed by other groups.[28] But in all of the above cases generally *t*-BuOOH or H_2O_2 are used as the oxidant in catalytic reaction which sometimes leads to chemical transformation of the UO_X nano species.[17,28] Therefore, to avoid or minimise the above mentioned problems, in our present case, using our synthesized uranium nanoparticles as catalyst we employed PhI(OAc)2 as a very simple but effective oxidant and EDC (ethylenedichloride) as the solvent employing the similar oxidation methods as reported by other groups using Mn2O3 as catalyst.[29]

The method of oxidation was followed as same as reported earlier. [29] The 1 mmol of the benzyl alcohol as the precursor was mixed with 0.01 mmol of the Urenium Oxide nanoparticles , 1.25 mmol of PhI(OAc)2 and 300 mg of the MgSO4 using 25 mL ethylenedichloride (EDC) as solvent. The resulting mixture was stirred in a magnetic stirrer maintaining 45°C temperature until the reaction reached completion. The conversion was monitored by doing TLC of the reaction mixture at a definite time interval. After completion of the reaction the mixture was filtered through a sintered funnel, the residue was collected and washed with the mother solvent (EDC). Then the combined filtrate was transferred in a separating funnel and extracted with water and the extract was collected over activated MgSO4 for absorption of excess moisture. The EDC was then evaporated under rotary evaporator. The

crude so collected was then further purified by column chromatography to obtain the aldehyde as the final product. EDC was used as the suitable solvent for the oxidation because the other solvents like water, methanol, ethanol, acetoniltrile, DCM, chloroform or THF are found to be not so much efficient for the conversion. The schematic representation of the alcohol oxidation was represented in the following scheme.

Scheme 2.

First the benzyl alcohol was used as substrate for the oxidation purpose using UNP1 to UNP4 as the catalyst. Among the obtained U_3O_8 nanoparticles, UNP1 and UNP2 displays significant activities for the catalytic oxidation of benzyl alcohol into benzaldehyde compared with the other two nanoparticles (UNP3 and UNP4). When the reaction achieves the maximum time (i.e. 8 hr) the UNP2 leads to 60% oxidation of benzyl alcohol, where as the UNP1 shows 55% oxidation. The other nano particles UNP3 and UPN4 shows 30% and 35% conversion respectively. Here conversion of the benzyl alcohol has been plotted against the reaction time at 45°C (Figure 7). To demonstrate the recyclability of the catalyst the experiments were repeat about five times as described in later section.

Fig. 7

To further analyse the higher catalytic activity of UNP2 among the others, the textural properties *i. e.* surface area of all the four nano particles were investigated by Brunauer–Emmett–Teller (BET) gas-sorption measurements performed at 77 K for the as-dried powder sample under vacuum, as shown in Fig. S19. The BET adsorption isotherm for the determination of surface area of finely divided solid is given by according to the following equation [30].

$$\frac{1}{W\left((P_0/P)-1\right)} = \frac{1}{W_mC} + \frac{C-1}{W_mC}\left(\frac{P}{P_0}\right) \quad \text{……………………..(1)}$$

Where, W= weight of gas adsorbed, P/P_0 = relative pressure, Wm = weight of adsorbate as monolayer, C = BET constant. From the plot of *1/(W((Po/P)-1)) vs P/P₀* the specific surface area of UNP2 (30.02 m^2/gm) and UNP1 (27.35 m^2/gm) is found to be higher than UNP3(15.37m^2/gm) and UNP4 (16.55 m^2/gm). Generally, it is considered that the higher the surface area, the higher is the catalytic performance if the same material is used as a catalyst. This corroborates well with the

experimental data obtained from the benzyl alcohol oxidation. As UNP2 has the smallest size and highest surface area according to the TEM analysis and BET data, so it is reasonable why it becomes the most efficient catalyst among the rest. The good catalytic activity of the UNP2 was further estimated employing various types of alcohols under the above mentioned reaction conditions (Table 4). The benzyl alcohols having activated and deactivated groups were used as substrates in this oxidation to obtain the aldehyde as the main product. And negligible amount acids as side product are also obtained (Table 4). Amusingly, it is observed that the deactivated alcohol demonstrating the highest rate of conversion over the other activated and normal benzyl alcohol as also reported in case of Mn_2O_3 nano particles by others[29].

Table 4.

3.7. Reusability and Recyclability of the Nanoparticles as Catalyst

The recycling effectiveness *i.e* reuse in several cycles is an important criterion for an excellent catalyst. For this very purpose we have chosen benzyl alcohol as a substrate and UNP2 as catalyst as a representative case for these recycling experiments. After each reaction cycle the catalysts are recovered and then washed thoroughly with acetonitrile and dried at 100°C for 2h. At the end of the 5th cycle the used catalyst has been further characterized by Powder XRD study, Scanning electron microscopy as well as by Transmission electron microscopy (**Fig. 8**). Comparing all the experimental results of the used catalyst with original one it is easy to conclude that no significant change has been takes place in the catalyst after oxidation reaction.Taking into account the catalyst loss during the recycling, the catalytic performance of the samples is quite stable, especially for the recycled samples. In other words the catalysts are recyclable as well as reusable.

Fig. 8

4. Conclusions

We successfully synthesized U_3O_8 nanoparticles form four different Uranyl-Schiff-base complexes in high yields through a facile pyrolytic route. The prepared U_3O_8 nanoparticles showed different morphological shapes with average size ranges of 50-100 nm. Catalytic testing revealed that the catalytic activity of the porous U_3O_8 nanoparticle (UNP2) was distinctly superior to that of other U_3O_8 nanoparticles for the oxidation of various alcohols to corresponding aldehydes.

The present results propose that the catalytic performance of U_3O_8 nanoparticles is morphology-dependent.

Acknowledgement

References

[1]   C. Burda, X. Chen, R. Narayanan, M. A. El-Sayed, Chem. Rev. 105 (2005) 1025.

[2]   V.Polshettiwar, J.M. Basset, ChemSusChem. 5 (2012) 6.

[3]   B. C. Ranu, D. Saha, D. Kundu, N. Mukherjee, Wiley-VCH. (2013).

[4]   R. S. Varma, Sustainable Chem. Processes. 2 (2014) 11.

[5]   Z. Chen, Z. Jiao, D. Pan, Z. Li, M. Wu, C.H. Shek, C. M. L. Wu, K. L. L. Joseph, Chem. Rev. 112 (2012) 3833.

[6]   W. Weifeng, C. Xinwei, C. Weixing, G. I. Douglas, Chem. Soc. Rev. 40 (2011)1697.

[7]   O. Giraldo, S. L. Brock, W. S. Willis, M. Marquez, S. L. Suib, S. Ching, J. Am. Chem. 427 Soc. 122 (38) (2000) 9330.

[8]   V. Polshettiwar, B. Baruwati, R. S. Varma, ACS Nano. 3 (2009) 728.

[9]   Z. Hao, C. Gaoping, W. Zhiyong, Y. Yusheng, S. Zujin, G. Zhennan, Nano Lett. 8 (2008) 430 2664.

[10]   Y. Hirao, C. Yokoyama, M. Makoto, Chem. Commun. (1996) 597.

[11]   E. A. Kotomin, Y. A. Mastrikov, E. Heifets, J. J. Maier, Chem. Chem. Phys. 10 (2008)

433 4644.

[12]   G. J. Hutchings, C. S. Heneghan, I. D. Hudson, S. H. Taylor, Nature. 384 (1996) 341.

[13]   S. H. Taylor, C. S. Heneghan, G. J. Hutchings, I. D. Hudson, Catal. Today. 59 (2000)
       436 249.

[14]   K. Vidya, S. E. Dapurkar, P. Selvam, S. K. Badamali, D. Kumar, N.M. Gupta, J. Mol.
       438 Catal. 181 (2002) 91.

[15]   T. Campbell, M. A. Newton, V. Boyd, J. Phys. Chem. B. 109 (2005) 2885.

[16]   H. Madhavaram, H. Idriss, J. Catal. 224 (2004) 358.

[17]   Q.Wang, G-D. Li, S. Xu, J-X. Li, J-S Chen, J. Mater. Che. 18 (2008) 1146.

[18]   Bruker (2005) SAINT v. 7.23; Bruker (2008) APEX; Bruker AXS Inc. Madison, Wisconsin,
       USA.

[19]   G.M. Sheldrick, *Acta Crystallogr.* A64 (2008) 112.

[20]   C.F. Macrae, P.R. Edington, P. McCabe, E. Pidcock, G.P. Shields, R. Taylor, , T. Towler, J.
       Streek, J. Appl. Cryst. 39 (2006) 453.

[21]   M. S. Bharara, K. Strawbridge, J. Z. Vilsek, T. H. Bray, A. E. V. Gorden, Inorg. Chem. 46
       (2007) 8309.

[22]   F. Valdivieso, M. Pijolat, M. Soustelle, J. Jourde, J. Sol. State Ionics. 117 (2001) 141.

[23]   F. Valdivieso, V. Francon, F. Byasson, M. Pijolat, A. Feugier, V. Peres, J. NuclearMaterials.
       354 (2006) 85.

[24]   Q. Wang, G. Dong Li, S. Xu, J. X. Li, J. S. Chen, J. Mater. Chem. 18 (2008) 1146.

[25]   J. Selbin, J. D. Ortego, Chem. Rev. 69 (1969) 657.

[26]   H. R. Hoekstra, S. Siegel, L. H. Fuchs, J. J. Katz, J. Phys. Chem. 59 (1955) 136.

[27]   Z. Tohidiyan, I. Sheikhshoaie, M. Khaleghib, J. Appl. Chem. 10 (2016) 71.

[28]   D. Kumar, R. P. Bhat, S. D. Samant, N. M. Gupta, Catal. Commun. 6 (2005) 627.

[29]   H. Rahaman, R. M. Laha, D. K. Maiti, S. K. Ghosh, RSC Adv. 5 (2015) 33923.

[30]   S. Brunauer, P. H. Emmett, E. Teller, J. Am. Chem. Soc. 60 (1938) 309.
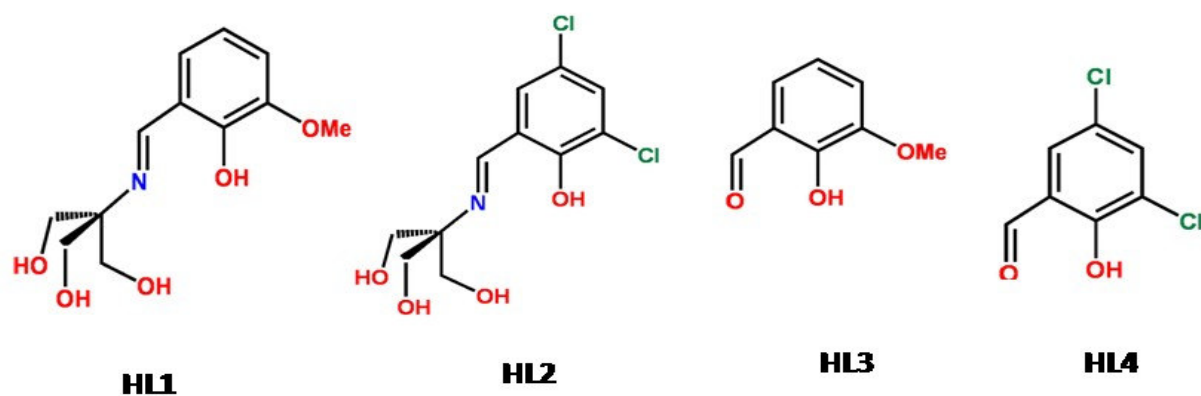
Scheme 1. Schematic representation of the four ligands.
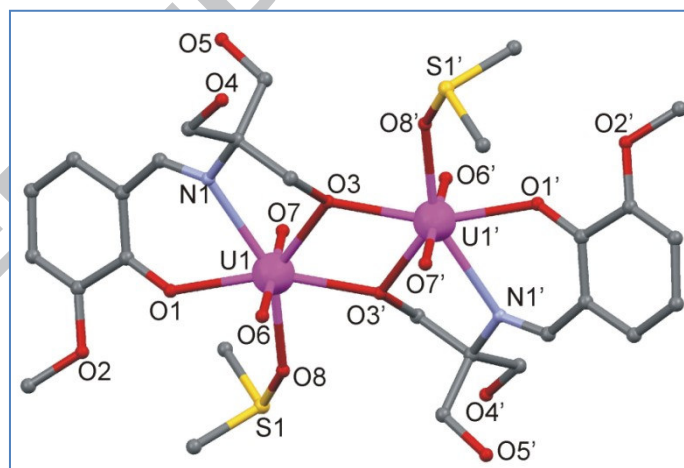
Fig. 1 Perspective view of a representative dinuclear unit of **1** together with the atom numbering scheme. Symmetry code: (') –x, 2-y,1-z
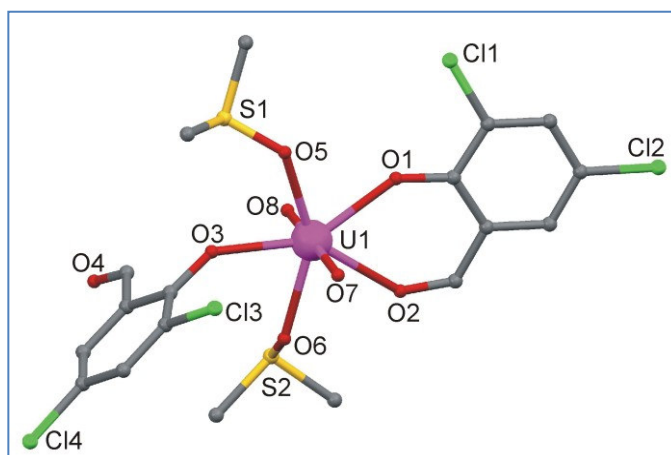
Fig. 2 Perspective view of **4** together with the atom numbering scheme.
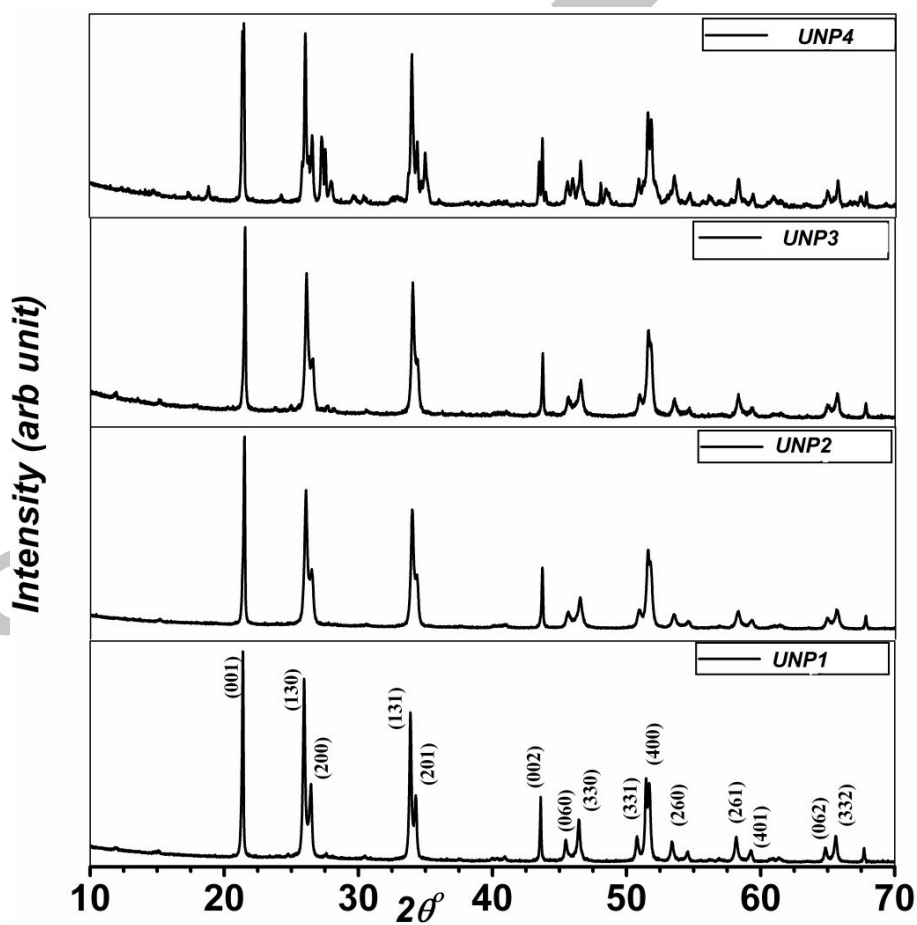
Fig. 3 Powder XRD pattern of different U_3O_8 nanoparticles.
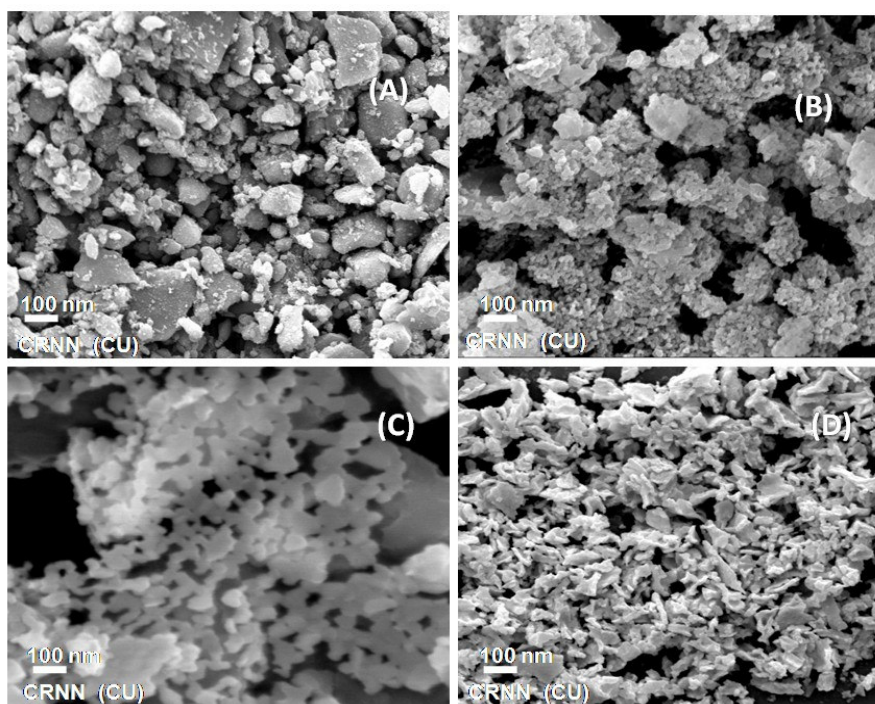
Fig. 4 Scanning Electron Micrograph images of (A) UNP1, (B) UNP2, (C) UNP3, (D)UNP4.
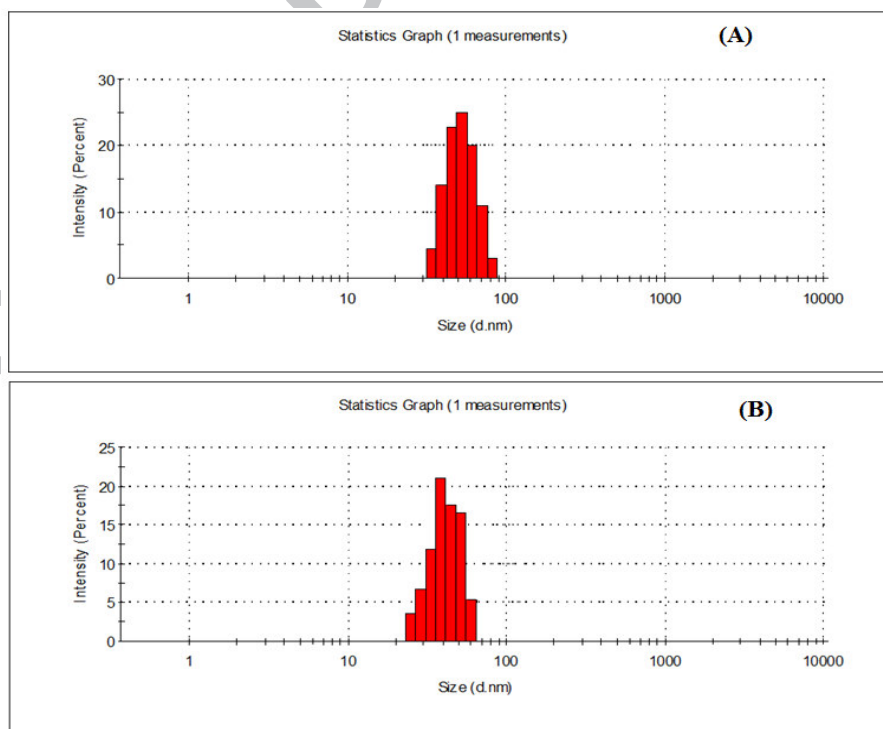
Fig. 5 Dynamic light scattering of (A) UNP1 and (B) UNP3
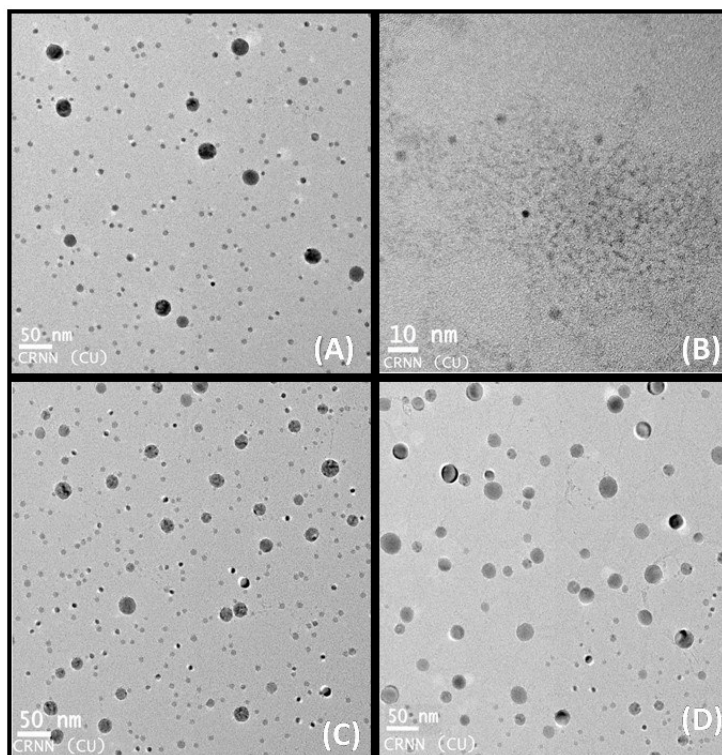
Fig. 6 Transmission electron microscopy images of (A) UNP1 (B) UNP2 (C) UNP3 (D) UNP4.
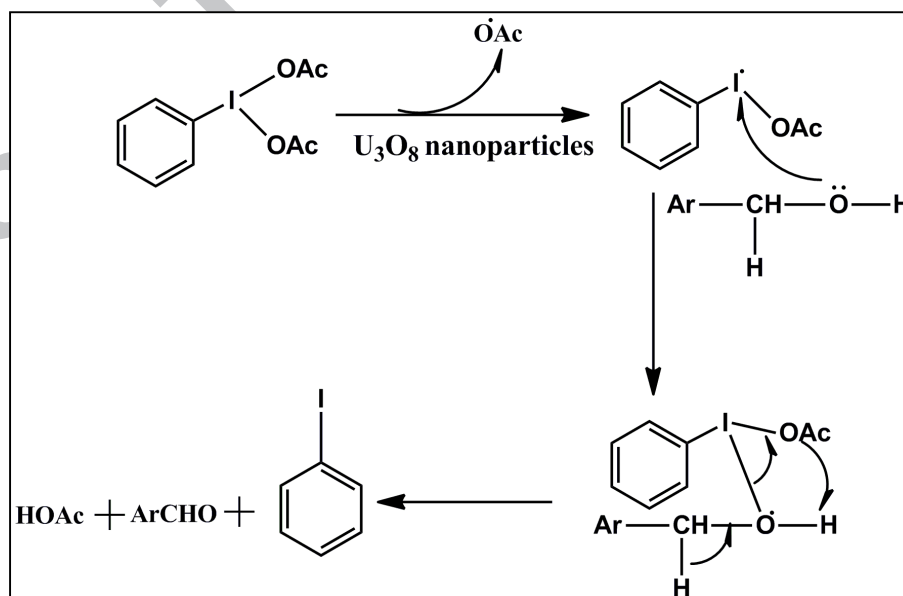
Scheme 2. Schematic representation of the alcohol oxidation.
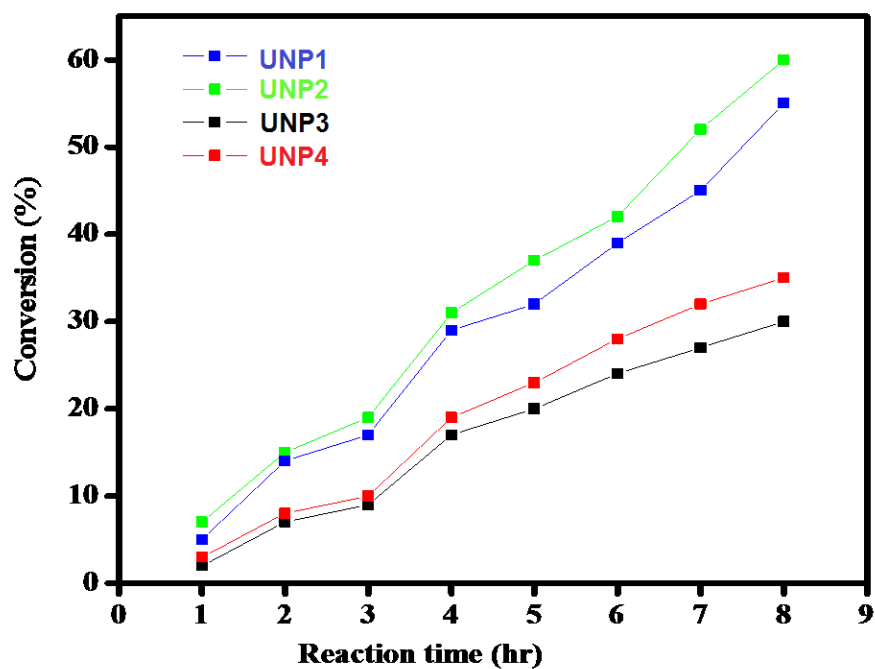
Fig. 7 The oxidation conversion of benzyl alcohol measured as a function of reaction time at 45°C using different uranium oxide materials as catalysts.
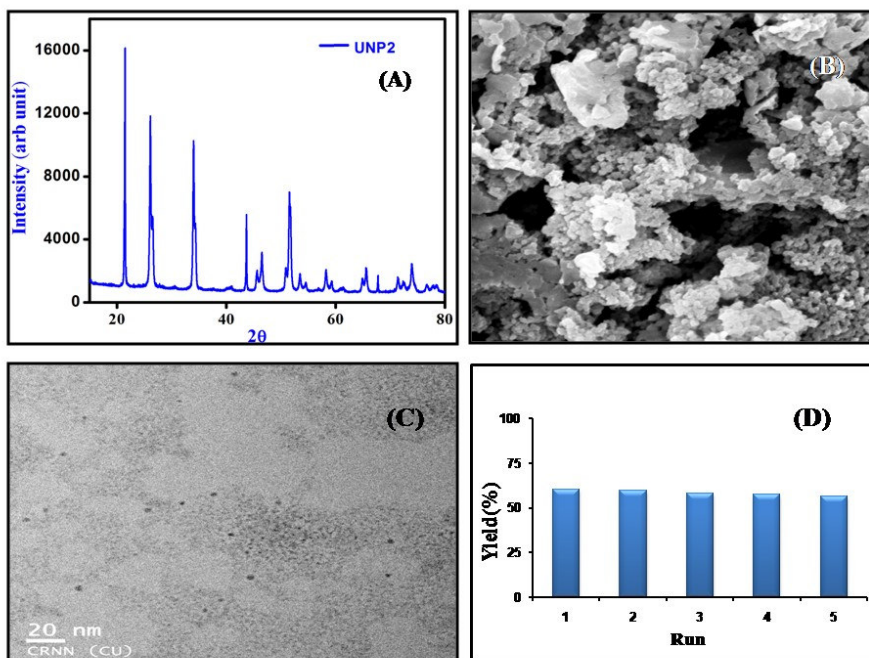
Fig. 8 Comparison data of oxidation of different alcohols by UNP2.

Table 1. Crystallographic Data and Details of Refinement for Complexes 1 and 4.

ound	1	4
rical formula	$H_{42}N_2O_{16}S_2U_2$	$_{8}Cl_4O_8S_2U$
ula mass	1202.82	39
m	triclinic	nic
e group	P-1	
	10.4511(5)	)6(2)
	16.9286(8)	-11(3)
	20.3307(9)	81(4)
	92.359(2)	351(1)
	91.594(2)	319(1)
	90.387(2)	31(1)
^{3})	3592.4(3)	32(6)
	4	
)	100(2)	2)
m^{-1})	9.194	)
Mg/m^3)	2.224	3
collected	18601	8
ue refl. / r_{int}	18601 / 0.000	/ 0.0263
meters / restraints	932 / 20	0
lness-of-fit on f^2	1.053	3
vr2 (all data)	0.0606 / 0.1630	3 / 0.0638
vr2 (confidence factors)	0.0898/0.1441	)6/0.0446
lual extrema (e/å^3)	3.94 / -5.22	/ -0.94

Table 2. Selected Bond Lengths (Å) and Angles (°) for Compound **1**.

U(1)-O(6)	1.792(9)	U(3)-O(31)	1.778(9)
U(1)-O(7)	1.813(10)	U(3)-O(30)	1.796(8)
U(1)-O(1)	2.278(7)	U(3)-O(25)	2.257(7)

U(1)-O(3')	2.341(7)	U(3)-O(27)	2.341(7)
U(1)-O(3)	2.351(7)	U(3)-O(27b)	2.356(7)
U(1)-O(8)	2.360(9)	U(3)-O(32)	2.383(9)
U(1)-N(1)	2.590(10)	U(3)-N(3)	2.589(11)
U(2)-O(14)	1.794(10)	U(4)-O(23)	1.793(9)
U(2)-O(15)	1.795(10)	U(4)-O(22)	1.797(9)
U(2)-O(9)	2.249(9)	U(4)-O(17)	2.260(9)
U(2)-O(11)	2.343(8)	U(4)-O(19)	2.336(9)
U(2)-O(11a)	2.352(9)	U(4)-O(19c)	2.359(9)
U(2)-O(16)	2.378(10)	U(4)-O(24)	2.368(10)
U(2)-N(2)	2.608(10)	U(4)-N(4)	2.577(10)
U(1)...U(1')	3.8930(7)	U(3)...U(3b)	3.8980(7)
U(2)...U(2a)	3.8707(8)	U(4)...U(4c)	3.8987(8)
O(7)-U(1)-O(6)	178.8(4)	O(7)-U(1)-O(8)	92.6(4)
O(6)-U(1)-O(1)	86.1(3)	O(8)-U(1)-O(1)	82.3(3)
O(7)-U(1)-O(1)	92.7(3)	O(8)-U(1)-O(3')	76.0(3)
O(6)-U(1)-O(3')	92.1(3)	O(8)-U(1)-O(3)	142.8(3)
O(3')-U(1)-O(7)	89.1(3)	O(6)-U(1)-N(1)	94.4(4)
O(3')-U(1)-O(1)	158.3(3)	O(7)-U(1)-N(1)	85.0(4)
O(6)-U(1)-O(3)	85.6(3)	O(1)-U(1)-N(1)	69.6(3)
O(7)-U(1)-O(3)	95.2(3)	O(3')-U(1)-N(1)	65.4(3)
O(3)-U(1)-O(1)	133.3(3)	O(8)-U(1)-N(1)	151.7(3)
O(3)-U(1)-O(3')	67.9(3)	O(6)-U(1)-O(8)	87.4(4)
O(3)- U(1)- N(1)	132.0(3)	O(7)-U(1)-U(1)	92.5(2)
O(6)-U(1)-U(2)	88.6(3)	O(1)-U(1)-U(2)	166.7(2)
O(3)-U(1)-U(2)	34.01(19)	O(3)-U(1)-U(2)	33.85(19)
O(8)-U(1)-U(2)	109.6(2)	N(1) –U(1)-U(2)	98.69(19)

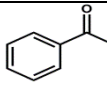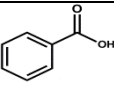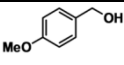Symmetry codes: (') –x,2-y,1-z; (a) 1-x,1-y,1-z; (b) 1-x,1-y,-z; (c) –x,1-y,-z.

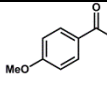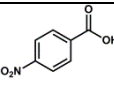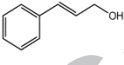**Table 3.** Selected Bond Lengths (Å) and Angles (°) for Compound **4.**

U(1)-O(7)	1.779(3)	U(1)-O(5)	2.367(2)
U(1)-O(8)	1.785(3)	U(1)-O(6)	2.402(2)
U(1)-O(3)	2.308(2)	U(1)-O(2)	2.517(2)
U(1)-O(1)	2.314(2)		
O(7)-U(1)-O(8)	175.73(11)	O(6)-U(1)-O(3)	75.73(8)

O(3)-U(1)-O(8)	90.11(11)	O(6)-U(1)-O(1)	137.47(8)
O(7)-U(1)-O(1)	90.89(10)	O(6)-U(1)-O(5)	148.86(8)
O(1)-U(1)-O(8)	89.88(10)	O(7)-U(1)-O(2)	85.82(10)
O(3)-U(1)-O(1)	146.79(8)	O(8)-U(1)-O(2)	90.56(11)
O(7)-U(1)-O(5)	90.96(10)	O(2)-U(1)-O(3)	144.63(8)
O(5)-U(1)-O(8)	93.29(11)	O(1)-U(1)-O(2)	68.58(8)
O(5)-U(1)-O(3)	73.19(8)	O(5)-U(1)-O(2)	142.02(8)
O(5)-U(1)-O(1)	73.65(8)	O(6)-U(1)-O(2)	68.94(8)
O(7)-U(1)-O(6)	87.97(10)	O(6)-U(1)-O(8)	88.63(10)
O(7)-U(1)-O(3)	91.54(10)		

Symmetry codes: (') –x,2-y,1-z; (a) 1-x,1-y,1-z; (b) 1-x,1-y,-z; (c) –x,1-y,-z.

Table 4. Catalytic activity of U_3O_8 nanoparticles using various alcohols as substrate.

Entry	Alcohol (1)	Catalyst	Reagent & conditions	Conversion (%)	Desired aldehyde (2)	Acid (3)	Yield (%, 2 : 3)
1.		UNP2 (0.01 mol %)	PhI(OAc)$_2$, EDC, 45 ℃ ,8.0 h	60	2a:58%	3a:2%	60 (29:1)
2.		UNP2 (0.01 mol %)	PhI(OAc)$_2$, EDC, 45 ℃ ,10.0 h	50	2b:56%	3b:4%	48 (14:1)
3.		UNP2 (0.01 mol %)	PhI(OAc)$_2$, EDC, 45 ℃ ,7.0 h	65	2c:55%	3c:5%	62 (11:1)
4.		UNP2 (0.01 mol %)	PhI(OAc)$_2$, EDC, 45 ℃ ,8.0 h	59	2d:56%	3d:4%	58 (14:1)
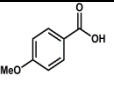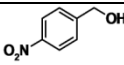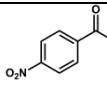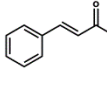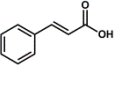
Graphical Abstract (Picture):
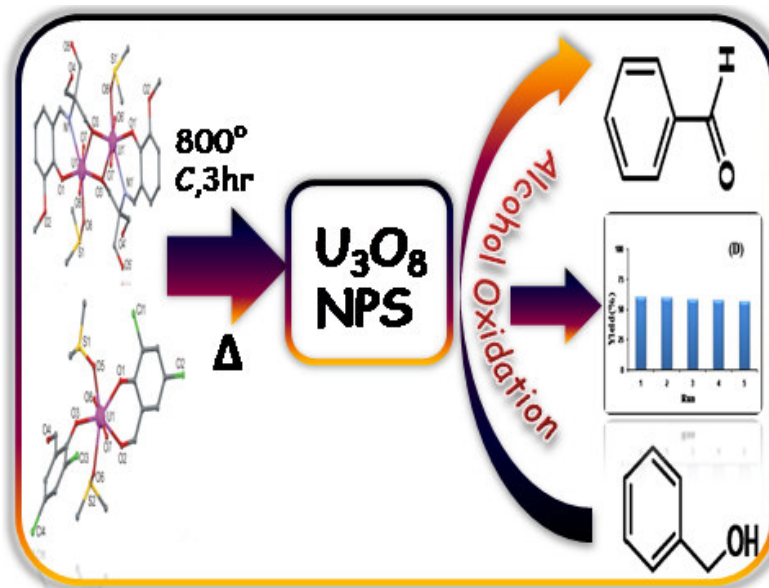
Graphical Abstract (Synopsis):

Four uranyl complexes have been synthesized and characterized, then undergone to pyrolytic reaction to produce U_3O_8 nanoparticles of different shape and morpholgy which affect their catalytic efficiency.

Highlights:

(1) Syntheses of Uranium Oxide nano particles by very simple but effective manner just by employing the pyrolytic reaction to our four synthesized complexes.

(2) Formation of U_3O_8 and UO_2 nano crystals from the respective precursors and then conversation of UO_2 to U_3O_8 nano materials of different shape and morphology.

(3) Well characterizations of the nano particles by means of X-ray diffraction (XRD), scanning electron microscopy (SEM), and transmission electron microscopy (TEM).

(4) Appreciable oxidation of benzyl alcohol by using $PhI(OAc)_2$ as a very simple but effective oxidant instead of regular t-BuOOH or H_2O_2, which minimizes formation of by-products and chemical transformation of the UO_x nano species.

(5) Finally four different U_3O_8 nanoparticles was explored as oxidising catalyst to oxidise alcohols where morphology of the nanoparticles controls the catalytic efficiency.